RESEARCH ARTICLE

Marek's disease virus influences the core gut microbiome of the chicken during the early and late phases of viral replication

Sudeep Perumbakkam[1,2], Henry D. Hunt[1] & Hans H. Cheng[1]

[1]Avian Diseases and Oncology Laboratory, USDA, ARS, East Lansing, MI, USA; and [2]Department of Animal Science, Purdue University, West Lafayette, IN, USA

Correspondence: Sudeep Perumbakkam, Avian Diseases and Oncology Laboratory, USDA, ARS, East Lansing, MI 48823, USA. Tel.: +517 337 6626; fax: +517 337 6776; e-mail: perumbak@msu.edu

Present address: Sudeep Perumbakkam, Department of Microbiology and Molecular Genetics, Michigan State University, East Lansing, MI 48824, USA

Received 25 March 2014; revised 17 July 2014; accepted 19 July 2014. Final version published online 26 August 2014.

DOI: 10.1111/1574-6941.12392

Editor: Julian Marchesi

Keywords
dysbiosis; microbiome; chicken; Marek's disease.

Abstract

Marek's disease (MD) is an important neoplastic disease of chickens caused by the Marek's disease virus (MDV), an oncogenic alphaherpesvirus. In this study, dysbiosis induced by MDV on the core gut flora of chicken was assessed using next generation sequence (NGS) analysis. Total fecal and cecum-derived samples from individual birds were used to estimate the influence of MDV infection on the gut microbiome of chicken. Our analysis shows that MDV infection alters the core gut flora in the total fecal samples relatively early after infection (2–7 days) and in the late phase of viral infection (28–35 days) in cecal samples, corresponding well with the life cycle of MDV. Principle component analyses of total fecal and cecal samples showed clustering at the early and late time points, respectively. The genus *Lactobacillus* was exclusively present in the infected samples in both total fecal and cecal bird samples. The community colonization of core gut flora was altered by viral infection, which manifested in the enrichment of several genera during the early and late phases of MDV replication. The results suggest a relationship between viral infection and microbial composition of the intestinal tract that may influence inflammation and immunosuppression of T and B cells in the host.

Introduction

With advances in next generation sequencing (NGS), there has been a substantial increase in our ability to identify and understand gastrointestinal (GI) tract-associated microorganisms, and their potential influence on human and animal health. For example, in human and mouse models, microorganisms have been shown to influence host immunity (Benson *et al.*, 2009) by producing certain small molecules that help regulate the immune system (Hooper *et al.*, 2000, 2001; Mazmanian *et al.*, 2005; Round & Mazmanian, 2010; Arpaia *et al.*, 2013), obesity (Ley *et al.*, 2005), inflammatory bowl disease (Mazmanian *et al.*, 2008), and colorectal cancer (Marchesi *et al.*, 2011).

Use of NGS technologies to answer objectives related to the influence of host immunity and microbiomes have also permeated into agriculturally relevant animal models such as the cattle rumen (Hess *et al.*, 2011) and swine gut (Kim *et al.*, 2012; Looft *et al.*, 2012). The GI tract represents one of the primary sites of exposure to pathogens. In this highly reactive environment, infections can threaten the homeostatic relationship between the host and its flora. Acute mucosal infections are also characterized by significant shifts in the microbiota, a phenomenon known as dysbiosis. Presently, the dysbiosis hypothesis suggests changes in health are due to alterations in the structure of the microbial community in the environment (Spor *et al.*, 2011). GI tract infections can also promote expansion of commensals with inflammatory potential, referred to as pathobionts that can directly exacerbate the pathological process (Egan *et al.*, 2012).

Marek's disease (MD) is a lymphoproliferative disease of chickens caused by Marek's disease virus (MDV; or Gallid herpesvirus 2). The virus targets lymphoid tissue such as the bursa of Fabricius, thymus, and spleen, where it infects B and T cells (Schat & Nair, 2008). The pathological characteristics of MD include mononuclear

FEMS MICROBIOLOGY ECOLOGY

infiltration of the peripheral nerves, gonads, iris, various viscera, muscles, and skin. Susceptible chickens develop $CD4^+$ T-cell tumors in visceral tissues and enlarged nerves resulting in paralysis, blindness, and eventually death. Due to the persistent nature of the virus in the feather dander shed from MDV-infected birds, all commercial chickens are exposed at a very early age. As a consequence, MD costs the worldwide poultry industry $1–2 billion annually due to condemnation of broilers (meat-type) and reduction in egg production in layers (egg-type) (Morrow & Fehler, 2004).

Little is known about the interaction of viruses on the microbiome, and is presently an area of active research in human and other animal models (Minot *et al.*, 2011). There is limited literature on the effects of MDV on gut-associated lymphoid tissue (GALT), the lymphoid tissue that is associated with the intestinal tract in chicken and a major regulatory of immune function associated with the GI tract. The chicken has several lymphoid tissues that are located in or close to the GI tract that play a role in the immunity of the bird. These immune lymphoid tissues include in addition to the pharyngeal tonsil, the bursa of Fabricius, thymus, and a number of diffused lymphoid tissues located in various regions of the GI tract such as the esophagus, proventriculus, duodenum, cervix, rectum, a pyloric tonsil, Peyer's patches, Meckel's diverticulum, and cecal tonsils (Lillehoj & Trout, 1996).

The objective of this study was to employ NGS on total fecal and cecal samples from individual birds during various times after viral infection to determine whether MDV infection causes dysbiosis in the core gut flora in chicken. And if there are changes in gut flora of the chicken, do these changes correspond to specific areas of the gut or specific genera? Results from this study would provide an initial basis for understanding the interaction between MDV and the chicken microbiome.

Materials and methods

Chicken and viruses

A total of 80 Avian Disease and Oncology Laboratory (ADOL) $15I_5 \times 7_1$ line, maternal antibody negative chicks (day 0) were randomly allocated to four Horsfall–Bauer (HB) units, with each unit containing 20 chicks. The HB units were in close proximity (uninfected and infected treatments) to each other to lessen environmental variation and room effects between the treatments. The HB was provided nonsterile air, which was devoid of particulates (negative pressure), and chicks were given free access to nonsterile antibiotic free food and water throughout the experimental time period. For the infected treatment group, 40 birds were injected in the peritoneum with 2000 PFU of MDV (Md5 strain, passage 7, a very virulent (vv) pathotype of MD) at day of hatch (0 day). The remaining 40 birds were classified as uninfected and served as controls. All experiments were approved by USDA-ADOL Animal Care and Use Committee (ACUC). The ACUC guidelines established and approved by the ADOL ACUC (April 2005) and the Guide for the care and use of Laboratory Animals by Institute for Laboratory Animal Research (2011) were closely followed throughout the experiments.

Chicken fecal and tissue sample collection

Two types of fecal sampling strategy were used for data collection. In the first strategy, total fecal samples (pooled from two HB with similar treatments) were collected every day from 2 to 7 days of age from uninfected and MDV-infected treatments. After this initial sampling period, total fecal sampling was done once a week for 4 weeks. For collecting total fecal samples, sterile weigh boats were left in isolators for a period of 4–6 h and bird droppings collected. Samples were pooled, homogenized, and a representative portion put into sterile 2 mL centrifuge tubes for storage at −80 °C.

The second fecal sampling strategy involved invasive sampling (cecal sampling) once a week starting at 14 days to end of the experiment (35 days). For invasive sampling, five random birds from each treatment were euthanized. The chicken cecum was sampled *c.* 2 cm above the cecal tonsils by making an incision. The contents of ceca were collected into a sterile tube containing lysis solution as previously described (Yu & Morrison, 2004). A second incision was made upstream to allow passing of lysis solution to remove adherent microorganisms from the ceca wall. Tubes were immediately frozen and stored at −20 °C.

Chicken tissue samples (spleens and ceca) were also collected from euthanized birds from each treatment and immediately stored in tubes containing RNAlater (Ambion, Austin, TX) and processed as per the manufacturer's protocol.

Birds that died during the nonsampling dates were examined via necropsy and scored for signs of MD, including tumors and nerve enlargement. Deaths within the first week of the experiment were classified as chick mortality.

Estimation of *in vivo* MDV replication by quantitative PCR (qPCR)

To validate the presence of MDV in the infected birds, quantitative PCR (qPCR) was performed on two tissue samples derived from invasive sampling of chicken. Total

DNA from chicken splenic and cecum tissue were isolated using the QIAamp DNA Mini kit (Qiagen, Valencia, CA) as per the manufacturer's protocol. Duplicate tissue samples were extracted for DNA, quantified using a Nanodrop ND-1000 (Thermo Fisher, Waltham, MA), and further verified by 1% agarose gel electrophoresis. The extracted tissue DNA was stored at −20 °C and used for all subsequent qPCR reactions.

Amplifications were performed using a multiplex PCR using the ABI 7500 Real-Time PCR System (Applied Biosystems Inc., Foster City, CA) using the TaqMan chemistry. Primers and probes used were previously designed (Gimeno *et al.*, 2008), and target MDV *UL27*, which encodes gB, and chicken *glyceraldehyde-3-phosphate dehydrogenase* (GAPDH). All 25 μL reactions consisted of 2.5–5 ng of template DNA, 1 pmol TaqMan probe, and 10 pmol of each primer. PCR was preformed in duplicates for every bird sample and results reported as the ratio of MDV gB copies per GAPDH copy, estimated using standard curves consisting of 10-fold serial dilutions of plasmids containing either MDV gB or GAPDH. Statistical analysis of qPCR analysis was performed using a 3-way ANOVA with a Tukey's HSD *post hoc* test by comparing Least Square (LS) Means between samples. *P* values were corrected for multiple corrections.

Microbial DNA extraction and PCR

Microbial DNA was extracted in duplicates from 50 to 75 mg of starting fecal or cecum material for each extraction using a protocol comprising of bead beating and column purification (Epoch Life Sciences, Sugar Land, TX), as previously described (Yu & Morrison, 2004). All reagents used in the DNA extraction were either made as per the described protocol (Yu & Morrison, 2004) or commercially obtained (Qiagen), and replaced at appropriate steps. DNA was quantified using a Nanodrop ND-1000 (Thermo Fisher), and run on a 1% agarose gel to verify and DNA from samples were combined and used for all subsequent PCR amplifications.

The V6 hypervariable region of the 16S rRNA gene was used as a marker for amplifying the chicken microbial population. The primers and protocol for amplifying the 16S rRNA-V6 gene marker have been described previously (Gloor *et al.*, 2010). The modified platform specific amplification primers for the Ion Torrent sequencer (Life Technologies, Grand Island, NY) was synthesized that contained a unique 8-mer oligonucleotide tag (Hamady *et al.*, 2008) attached to the reverse primer. To generate amplicons for sequencing, a single step 25 μL PCR was performed for each sample and time point that contained *c.* 75–100 ng purified bacterial genomic DNA, 200 μmol dNTPs, 2.5 mM $MgCl_2$, 10 pmoles of each primer, and 0.25 units Phusion high-fidelity Taq polymerases (NEB, Ipswich, MA). Twenty PCR cycles were run on a PTC-200 thermocycler (MJ Research Inc., Watertown, MA). All PCR reactions were carried out in duplicates and visually confirmed by agarose gel electrophoresis. Individual barcoded PCR products were purified, quantified using a Nanodrop ND-1000 (Thermo Fisher), and then combined at equimolar concentrations for sequencing.

A 318 Ion Torrent chip (Life Technologies, Guilford, CT) was used to perform the amplification at the Michigan State University Research Technology Support Facility (www.rtsf.msu.edu). An emulsion PCR was setup for 100 cycles and the final FASTQ format file was then used for analysis of the data.

Phylogenetic analysis

Sequence analysis was performed using Mothur (version 1.30.2) (Schloss *et al.*, 2009) and Quantitative Insights into Microbial Ecology (QIIME) pipelines (version 1.7.0) (Caporaso *et al.*, 2010b) using default parameters, unless otherwise noted. Using Mothur, Ion Torrent-derived FASTQ sequences were first screened for quality using the following parameters: minimum quality score of 25, minimum sequence length of 50 bp, no ambiguous bases in the entire sequence, and up to one mismatch in the primer sequence. Reads not meeting these parameters were excluded from downstream analyses. Sequences were then sorted by barcode into respective samples, and the barcode and primer sequences trimmed from the FASTQ files. Sequences were renamed using a custom Perl script and the resulting FASTA sequences then imported to QIIME for further analysis. The sequences were assigned operational taxonomic units (OTUs) using the reference with *de novo* based approach using UCLUST (Edgar, 2010) at 97% identity against the Greengenes database (version 13.4) (DeSantis *et al.*, 2006). A representative sequence for each OTU was chosen as the centroid of each cluster, and these representative sequences were aligned using PyNAST (Caporaso *et al.*, 2010a). A phylogenetic tree was constructed using the FastTree program (Price *et al.*, 2009) for use in phylogenetic diversity calculations. Taxonomy was assigned using naïve Bayesian RDP classifier (Wang *et al.*, 2007) against the Greengenes database at a 0.50% similarity from the reference set on the basis of identification as chimeric via ChimeraSlayer.

Alpha diversity was computed using the full data set at a sampling depth of 14 780 sequences per sample in the total feces (pooled) and 4543 sequences for individual bird ceca samples at each time point. Bray–Curtis and UniFrac (Lozupone & Knight, 2005) (weighted) distances were computed between all samples at a similar subsampling.

Principal coordinates analysis (PCoA) was applied to visualize the differences between the infected and uninfected samples vs. days. Changes in bacterial abundance were compared using an ANOVA and two-tailed Student's *t*-test to find significance of OTU estimates. Bonferroni correction was applied in all statistical tests to account for multiple comparisons.

Results

Quantification of MDV in chicken tissues

MDV genomes were detected in the infected birds sampled at 14, 21, 28, and 35 dpi (Fig. 1) by qPCR. A 3-way ANOVA was performed to test for statistical differences in MDV copy numbers between the sampling time points and tissue types (spleen vs. ceca). The age-matched uninfected birds were negative for the presence of MDV in both tissue types ($P < 0.001$). Moreover, both splenic and ceca samples showed detectable copies of MDV at all sampling points but with no statistical correlations between tissue types. The differences in MDV copy numbers were significantly different between the splenic and cecal tissue samples ($P < 0.001$), with splenic tissue having greater copies at 14 dpi. There were differences in the relative copies of MDV over the sampling time period, which was influenced by the tissue type. For example, day 14 splenic tissues had significantly more copies of MDV over other splenic tissue for all time points or tissue types ($P < 0.001$).

Alpha and beta diversity of total feces in uninfected and MDV-infected birds

For the total feces, a minimum sampling size of 14 780 sequences per time point/treatment was used for the estimation of OTUs, alpha diversity, and beta diversity. At the phyla level, irrespective of treatment or days, the total sequences in uninfected (Supporting Information: Fig. S1a) and MDV-infected (Fig. S1b) treatments were classified into three major phyla, namely *Firmicutes*, *Proteobacteria*, and *Cyanobacteria*. In the uninfected treatment (Fig. S1a), an average of 72% and 16% of the sequences were classified as either phylum *Firmicutes* or *Proteobacteria*, respectively. The relative abundance of sequences assigned to phylum *Firmicutes* ranged from a maximum 13 678 sequences or 97.73% on day 2 to a minimum of 2156 sequences or 15.47% on day 7. Phylum *Proteobacteria*, the second most abundant phyla, ranged from 14 to 11 410 sequences, with the lowest percentage (0.10%) on day 2 and highest percentage represented at day 7 (81.50%), respectively. Phylum *Cyanobacteria*, the third highest phyla had a range of 42–3206 sequences with percentages ranging from 0.03% (day 35) to 22.90% (day 6), respectively.

In the infected treatment, (Fig. S1b), an average of 75% of the sequences at all days were classified as phylum *Firmicutes* with the highest number of *Firmicutes* sequences associated at day 14 (13 651 or 94.80%). Phylum *Proteobacteria*, the second most abundant group in the infected treatment, ranged from 144 to 11 116

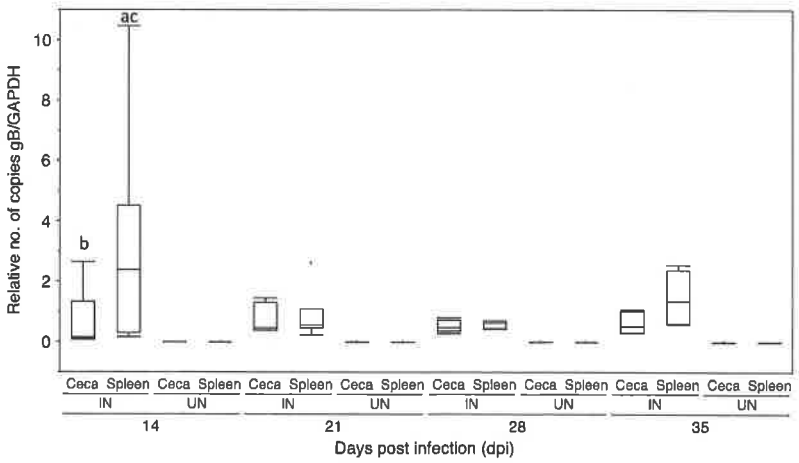

Fig. 1. Relative copy numbers of MDV genomes in splenic and cecum chicken tissues at 14, 21, 28, and 35 days postinfection (dpi) as measured by qPCR. IN represents the infected samples and UN represents the uninfected samples. Data are represented as outlier boxplots with whiskers that represent 1.5× interquartile range (IQR) and potential outliers are represented as black points. A 3-way ANOVA was used to determine statistical differences between the dpi, tissue types, and status of infection and significance is represented by the presence of an alphabet on the sample. 'a' represents significant difference on MD genome copy number between spleen samples on sampling days (infected vs. uninfected) across all days. 'b' represents the significant differences between the ceca samples (infected vs. uninfected) across all days, and 'c' represents significant differences between the two tissues spleen and ceca across at 14 dpi time point.

sequences ranging from 1.00% at 21 days to 77.20% at 2 days. Day 5 had the highest number of sequences (849 or 5.30%) associated with phylum *Cyanobacteria* that went down to 43 (0.30%) on day 7.

The rate and order of colonization of the two dominant phyla, *Firmicutes* and *Proteobacteria*, were inverse to each other in the uninfected and infected treatments between 2 and 7 days (Fig. S1). In the uninfected treatment, there was early colonization by phylum *Firmicutes* on day 2, with progressive increase in sequences associated with phylum *Proteobacteria* over the sampling time, which peaked at 7 days. In contrast, in the infected treatment, initial colonization was associated with phylum *Proteobacteria* and was gradually replaced by sequences associated with phylum *Firmicutes*. This phenomenon was observed only during the first 7 days, after which there appeared to be no differences in the colonization in the total fecal samples.

As there were no significant differences at the phyla level, a more detailed analysis on the genera level differences were performed. At the genus level, the sequences were classified at 97% sequence identity into *c.* 175 OTUs, of which genera ≥ 1% in either treatment (uninfected and infected) was used for further analysis (Fig. 2a and b). At the ≥ 1% representation, 21 OTUs were represented in uninfected or infected treatment and the remainder sequences were reclassified as 'Genera_Other'. Although the majority of the genera were present in both uninfected and infected treatments, there were exceptions as a few genera were exclusively present in one or the other treatment. To observe changes in OTUs in relation to infection status, relative abundance, and age of birds, heatmaps were plotted with the data for uninfected (Fig. S2a) and MDV-infected treatments (Fig. S2b).

To identify changes in abundance levels of genera associated with the type of treatment, the data were reanalyzed and regrouped at both the phylum (data not shown) and genera level (Fig. 3) as early (2–7) days, middle (14–21) days, and late (28–35) days in uninfected and MDV-infected birds. Data analysis showed significant differences ($P < 0.005$) at the genera level among uninfected and MDV-infected samples across tissues and time samples (Table 1). This reclassification lead to three scenarios in which bacteria were found, namely (1) OTUs present in both treatments, (2) OTUs exclusive to either uninfected or infected, and (3) OTUs present in both treatments but at significantly different ratios. Five genera were found significant in the early time point, four in the middle, and one in the later time point. Moreover, genera *Sporosarcinia* and *Turicibacter* were significantly present in higher numbers in the middle time point compared with the early and late time points. Certain genera, such

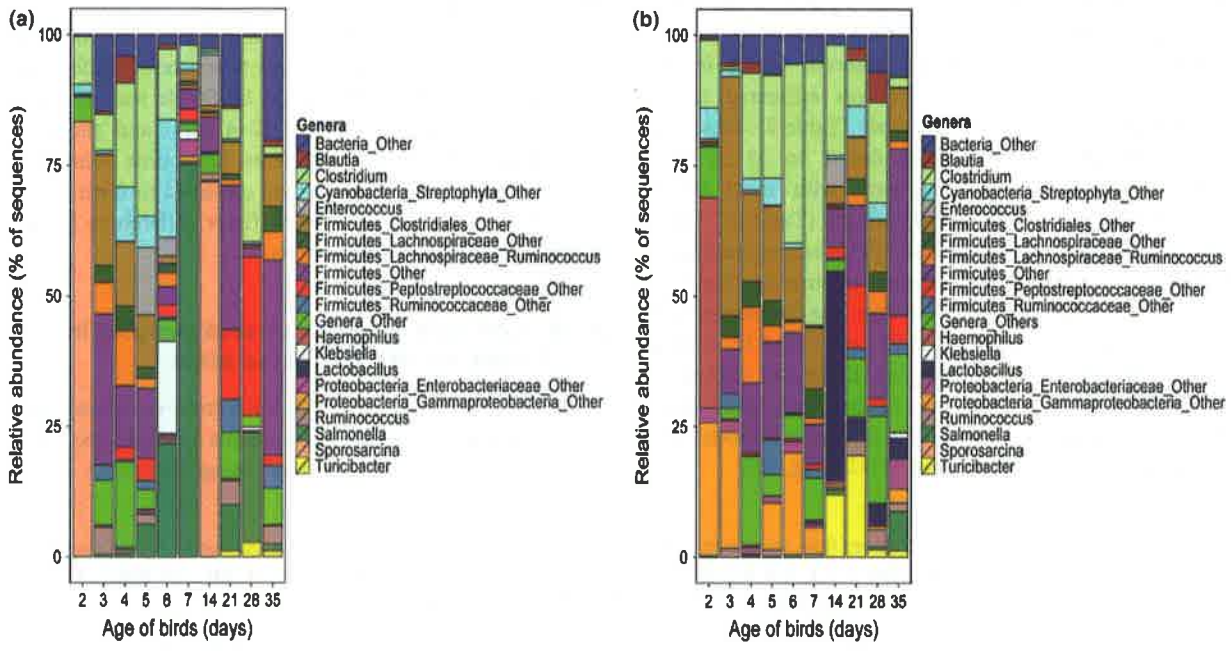

Fig. 2. Bacterial communities of total fecal samples from chicken at the phyla level. Data were analyzed using QIIME and phyla numbers ≥ 1% was plotted. The *x*-axis represents the sampling time points (days) and *y*-axis represents the relative abundance of sequences. Panel a) represents uninfected chicken total fecal samples, and panel b) are samples from chickens challenged with MDV and days represent, days postinfection (dpi).

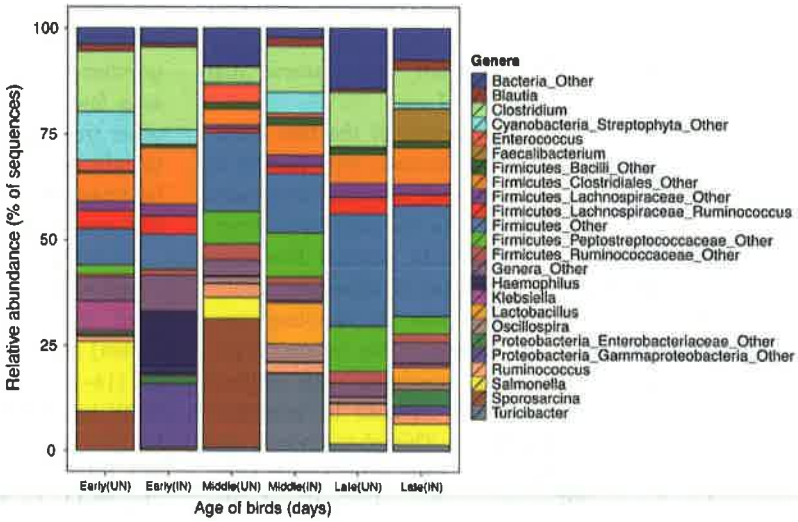

Fig. 3. Bacterial communities of total feces from chicken recategorized as early (2–7 days), middle (14–21 days), and late (28–35 days) time points in uninfected and MDV-infected samples at the genera level. Data were analyzed using QIIME and genera ≥ 1% were plotted. The *x*-axis labels describe the treatment uninfected (UN) or MDV-infected (IN) and the *y*-axis represents relative abundance at sequences as percentages.

as *Haemophillus* (8.00%) and *Lactobacillus* (3.80%) were present exclusively in the infected treatment and *Sporasarcina* (11.30%) was exclusive to the uninfected treatment. Certain genera were present in higher ratio between the two treatments. For example, *Salmonella* represented 13.30% of the sequences in the uninfected treatment but were present at a small percentage (0.90%) in the samples from infected birds. *Turicibacter* and sequences associated with associated *Gammaproteobacteria* were higher in the infected (5.90% and 8.40%) when compared to the uninfected treatments (0.20% and 0.30%), respectively.

The total average number of observed OTUs in the uninfected and infected samples was estimated to be 928.88 and 957.06 OTUs, respectively (Table 2). Observed OTUs gradually increased from day 2 to 35 in both infected and uninfected treatments, with most OTUs found on day 35 in the infected sample (Table 2). There were no correlations in increased OTUs corresponding to days in the uninfected and infected treatments (Fig. S3). The average estimated OTUs between the uninfected and infected treatments were 2156.95 and 2012.12 OTUs, respectively (Table 1); showing no significant difference in the OTU estimate based on control and MDV challenged birds. The estimated OTUs showed a bimodal distribution similar to the observed OTUs (Fig. S4).

PCoA using Bray–Curtis distances calculated using QIIME of 14 780 sequences per sample showed that the uninfected and infected communities start off as different communities during the early (2–7 days) colonization process (Fig. 4, group 1). As time progressed (14–35 days), the infected community became more similar compared to the uninfected treatment (Fig. 4, group 2). To see whether relative abundances of OTUs played a part in the clustering patterns rather than the presence or absence, weighted UniFrac analysis was performed (Fig. S5). The early time points (2, 3, and 4 days) in both the uninfected and infected treatments clustered differently showing that relative abundance of OTUs was different between the early time period (2–4 days) and the later time period between the treatments. Later time points did not show differences and the data clustered to form a single group suggesting there were fewer differences in the abundance within the treatments.

Alpha and beta diversity of ceca samples in uninfected and MDV-infected birds

At 14, 21, 28, and 35 days, five birds from each treatment were invasively sampled and contents of their ceca collected, DNA extracted, amplified using 16S rRNA gene–

Table 1. ANOVA analysis of total feces obtained from uninfected and MDV-infected birds regrouped as early (2–7 days), middle (14–21 days), and late (28–35 days) time periods. Both within time period and across time period analysis was performed and data reported are significant OTUs ($P < 0.005$) after Bonferroni correction for multiple testing. * Indicates across time-point significant OTUs.

Early (2–7 days)		Middle (14–21 days)		Late (28–35 days)	
Uninfected	Infected	Uninfected	Infected	Uninfected	Infected
Salmonella	*Firmicutes_Clostridiales_*Other	*Sporosarcina**	*Turicibacter**		*Faecalibacterium*
Sporosarcina	*Proteobacteria_Gammaproteobacteria_*Other		*Lactobacillus*		
	Haemophilus		*Clostridium*		

Table 2. Phylogenetic analyses of MDV uninfected and infected birds at days post infection (dpi) of total fecal samples. Estimated, observed OTUs, Shannon, and Simpson indices were calculated at 97% using QIIME and tabulated

DPI	Treatment	Estimated OTU's	Observed OTU's	Shannon Index	Simpson Index
2	Infected	1413.68	638.40	3.75	0.78
2	Uninfected	849.75	449.90	2.04	0.42
3	Infected	1995.27	875.50	4.73	0.88
3	Uninfected	2513.98	1107.20	6.24	0.95
4	Infected	2133.21	895.60	6.16	0.96
4	Uninfected	2260.26	946.00	6.12	0.96
5	Infected	2608.95	1029.20	5.82	0.95
5	Uninfected	2766.41	1075.20	5.86	0.94
6	Infected	1830.81	817.00	4.59	0.88
6	Uninfected	2079.58	932.10	5.73	0.94
7	Infected	1978.32	1036.70	5.50	0.89
7	Uninfected	1840.34	839.40	4.10	0.78
14	Infected	1542.34	718.40	4.31	0.82
14	Uninfected	1327.05	653.70	3.03	0.57
21	Infected	2426.65	1019.00	6.60	0.96
21	Uninfected	2564.04	1142.60	6.71	0.96
28	Infected	2747.39	1271.70	7.46	0.97
28	Uninfected	1148.94	597.70	3.69	0.82
35	Infected	2892.85	1269.10	6.42	0.95
35	Uninfected	2770.88	1545.00	7.68	0.98

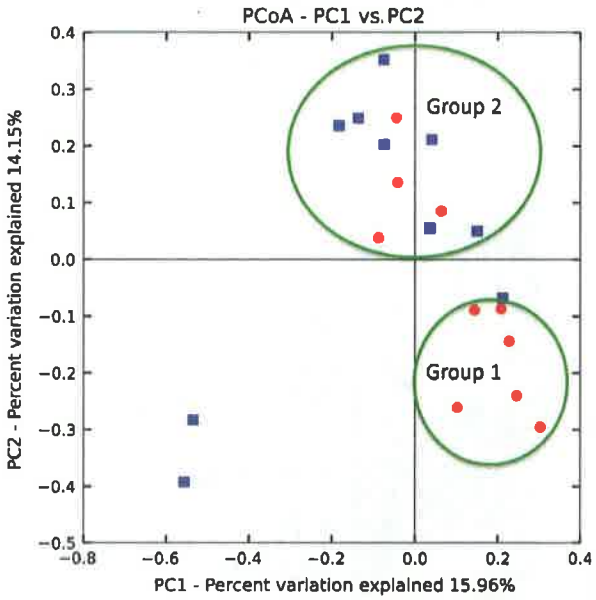

Fig. 4. PCoA analysis of total fecal samples of chicken when challenged with MDV. Blue squares represent uninfected samples and red circles represent infected samples. Group 1 represents the early 2–7 days sampling time periods in the infected samples and group 2 represents the clustered time points (14, 21, 28, and 35 days) in both uninfected and MDV-infected samples.

V6 primers, sequenced, and the data analyzed as described. A total of 4543 sequences from each bird sample/time were used for the classification and analysis process. At the phyla level, irrespective of treatment or days, the total sequences from individual bird samples (Fig. S6) in uninfected and MDV-infected treatments, or from data averaged by time point (Fig. 5), were classified into major phyla, namely *Firmicutes* and *Proteobacteria*, with few belonging to unclassified bacteria represented as 'Bacteria_Other'. The relative abundance of phylum *Firmicutes* ranged from *c.* 33.90% to 85.50% in the uninfected treatment and from 65.30% to 94.60% in the infected treatment. Phylum *Proteobacteria* ranged from 0.10% to 58.60% in the uninfected and 0.00% to 24.70% in the infected treatments. There was a sizeable portion of unclassified bacterial sequences in both uninfected (6.40–24.70%) and infected (5.30–30.40%) treatments, respectively.

At the genus level, 4543 sequences were classified at 97% sequence identity into *c.* 65 OTUs of which OTUs ≥ 1% in either treatment (uninfected or infected) was used for further analysis (Fig. S7). At the ≥ 1% representation, 16 OTUs were represented in uninfected or infected treatment, and the reminder were reclassified as 'Genera_Other'. Heatmaps were used to visualize the patterns of abundance and occurrence of OTUs in both uninfected (Fig. S8a), and infected treatment (Fig. S8b) in the cecum.

To identify abundance level of genera associated with the type of treatment, the data were reanalyzed and regrouped as mentioned in the total fecal sample analysis section. The days were regrouped with sampling days 14 and 21 regrouped as middle and days 28–35 was grouped

Table 3. Phylogenetic analyses of MDV uninfected and infected birds at 14, 21, 28, and 35 days post infection (dpi) in cecum samples. Estimated, observed OTUs, Shannon, and Simpson indices were calculated at 97% using QIIME and tabulated

DPI	Treatment	Estimated OTU's	Observed OTU's	Shannon Index	Simpson Index
14	Infected	904.86	441.47	5.95	0.93
14	Uninfected	879.57	438.95	5.94	0.94
21	Infected	632.19	339.62	5.10	0.91
21	Uninfected	734.54	406.20	5.82	0.93
28	Infected	776.88	407.20	5.72	0.93
28	Uninfected	1023.11	538.47	6.76	0.97
35	Infected	1003.36	517.70	6.37	0.95
35	Uninfected	996.27	520.13	6.71	0.97

as the late time point, similar to the total fecal analysis as middle and late time points (Fig. 6). Most genera were present in both the uninfected and infected treatments except for genus *Lactobacillus* (3.10%), which was present exclusively in the infected treatments. Certain genera were present in higher ratios between the two treatments. For example, genus *Faecalibacterium* represented 6.20% of the sequences in the late time point but was present at a small percentage (1.50%) in the corresponding uninfected time point.

The total average number of observed OTUs in the uninfected was estimated to be 414.66 and 531.95 in the middle and late time points, respectively (Table 3). In the infected treatment, a total of 390.58 in the middle and 454.92 OTUs in the late time point were observed. There were significant differences ($P < 0.05$) in the alpha diversity between middle and late time point between the uninfected treatments. Similar significance ($P < 0.05$) was observed between uninfected late and infected middle.

Estimated OTUs in the cecum ranged from 757.04 to 876.13 OTUs in the infected samples and from 769.67 to 1024.94 OTUs in the uninfected birds. There were significant differences in the estimated OTUs ($P < 0.05$) between uninfected middle and late time points. Diversity index such as the Shannon index was significant ($P < 0.05$) between uninfected middle and late, uninfected late and infected middle, and between infected late and uninfected late (data not shown).

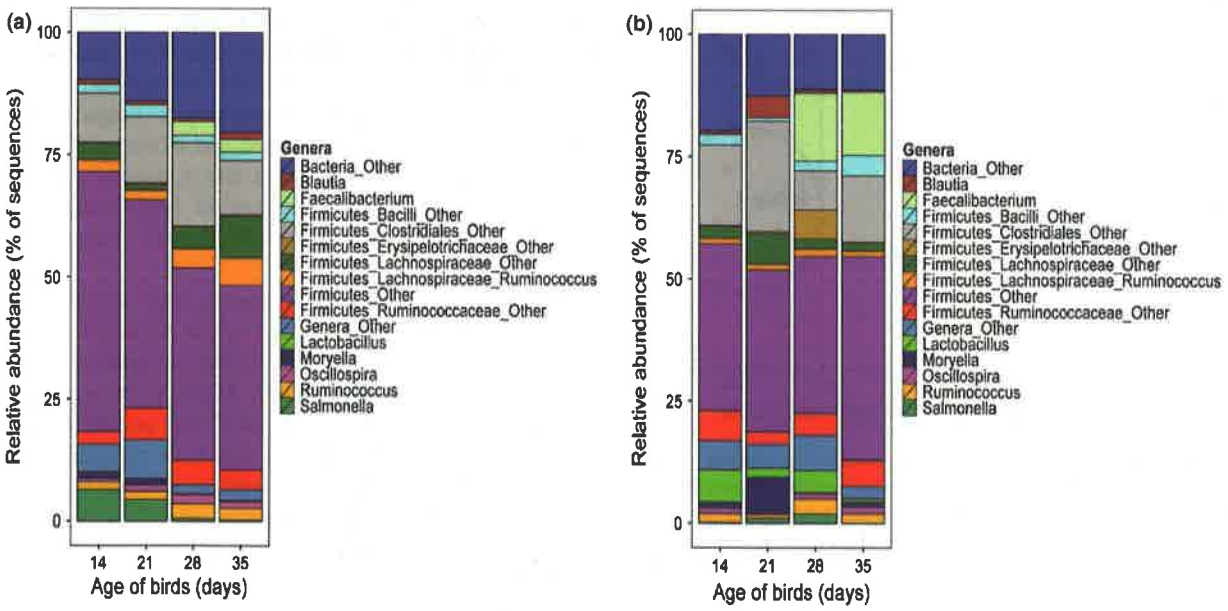

Fig. 5. Bacterial communities of cecum samples from chicken at the genera level. Data shown were averaged based off individual bird samples at 14, 21, 28, and 35 days time points in uninfected and MDV-infected samples using QIIME. Genera numbers ≥ 1% was plotted for both treatments and the *x*-axis labels describe the sampling time points. The *y*-axis represents relative abundance at sequences as percentages. Panel a) represents uninfected chicken samples at mentioned sampling points and panel b) are samples from chickens challenged with MDV and days represent, days postinfection (dpi).

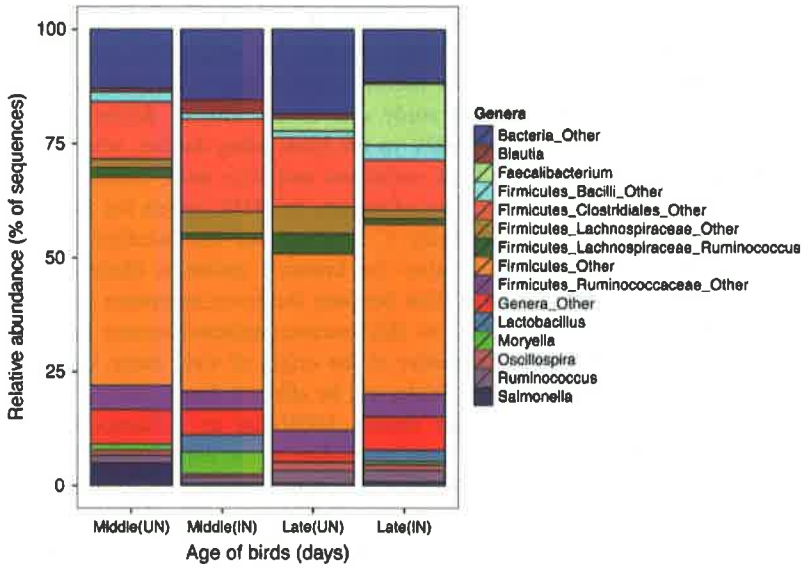

Fig. 6. Bacterial communities of cecum samples from chicken recategorized as middle (14–21 days) and late (28–35 days) time points in uninfected and MDV-infected samples at the genera level. Data were analyzed using QIIME and genera ≥ 1% were plotted. The *x*-axis labels describe the treatment uninfected (UN) or MDV-infected (IN), and the *y*-axis represents relative abundance at sequences as percentages.

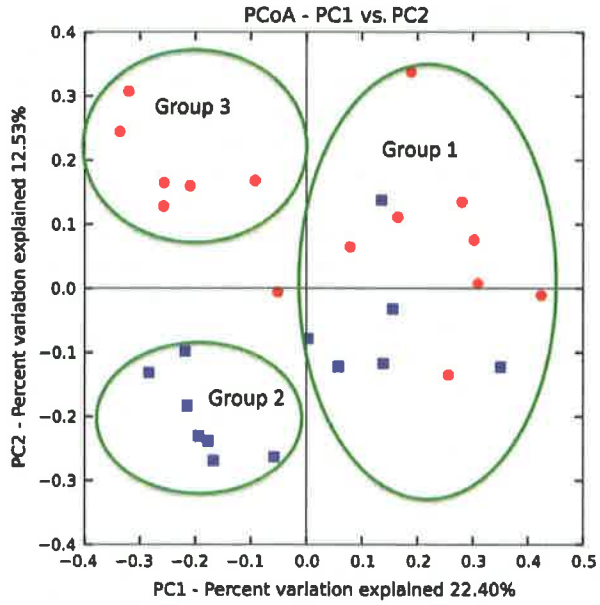

Fig. 7. PCoA analysis of cecum samples of chicken when challenged with MDV. Blue squares represent uninfected samples and red circles represent MDV-infected samples. Group 1 represents the middle sampling time periods (14–21 days) in the both the uninfected and MDV-infected samples, group 2 (red circles) represents the late time period (28–35 days) remaining in the MDV-infected samples, and group 3 (blue squares) represents the late time period (28–35 days) in the uninfected birds.

PCoA using Bray–Curtis distances calculated using QIIME of 4543 sequences per sample showed that the uninfected and infected communities harbor characteristic communities of bacteria that differ from one another (Fig. 7). The treatment days formed three groups. The first group consisted of 14- and 21-day samples from both uninfected and infected. As time progressed, the community shifted to form two other distinct groups, which represented the uninfected treatment (group 2) and the infected treatments (group 3) at 28 and 35 days, respectively.

The weighted UniFrac analysis (Fig. S9) showed no distinct pattern to the clustering between uninfected and infected treatments, validating that the presence/absence of certain genera were responsible for this shift in the cecal microbiome.

Discussion

There has been an increased focus to study the effect of immunity and its association with core gut flora using animal models (Atarashi *et al.*, 2013). This study represents one such attempt to define the effect of dysbiosis as a component of virus infection on the host microbiome in chicken.

On the microbial front, most available data on the community structure found in the chicken gut was acquired using traditional culture-based methods (Scupham, 2007). Based on available data, the chicken gut has flora comprised of bacteria (Scupham, 2007), methanogenic archaea (Saengkerdsub *et al.*, 2007), fungi (Okulewicz & Zlotorzycka, 1985), viruses (Qu *et al.*, 2008), and a few protists (Okulewicz & Zlotorzycka, 1985). Although these traditional culture-based studies have been done in past decade, there is good congruence with data generated using NGS techniques (Qu *et al.*, 2008). In general, the bacterial population of the chicken gut is mainly comprised of phyla *Firmicutes*, *Proteobacteria*, and *Bacteroides* (Qu *et al.*, 2008).

The GI tract represents one of the primary sites of exposure to pathogens (Molloy *et al.*, 2013) and the regulation of immunity. Chicks inoculated at day of hatch (0 days) and sampled for meconium, yielded no microbial load (data not shown) suggesting that birds are hatched sterile and colonization of the GI tract happens through environmental exposure such as air, feed, and water. Moreover based on the data, there is a possibility that the chicken gut is compartmentalized and colonized by different groups of bacteria. This is evident by the overlap of OTUs, between the total fecal and cecum populations. Fourteen OTUs overlapped between the two sampling tissues irrespective of time. Nine OTU's were exclusive to the total fecal samples, and surprisingly, 3 OTUs were found exclusive to cecum population (Fig. S10). Although the total fecal samples were sampled at higher number compared to cecum samples (14 780 vs. 4543 sequences), there was exclusion of few genera namely, Moryella and sequences associated with *Firmicutes_Erysipelotrichaceae*_Other, suggesting either there is a time based shedding behavior in chicken or these bacteria are attached to the cecum walls and do not disassociate. The rate of colonization in the uninfected chicken gut is bimodal (Fig. S4) suggesting that some internal metabolic/hormonal switch bottlenecks the abundance of bacteria at 7–14 day period, after which colonization continues normally. The exact mechanism or the causative action for this bottlenecking is unknown or unlikely could be a sampling anomaly. Although the uninfected controls at day 7 had sequences belonging to *Salmonella sp.*, independent analysis revealed that these sequences were not associated with *Salmonella pullorum,* a potential chicken pathogen.

Based on the 'Cornell Model' for the MDV life cycle (Calnek *et al.*, 1984b), MDV has a complex replication cycle and goes through four phases namely, early cytolytic phase (2–7 days), latent phase (7–10 days), late and immune suppressive phase (18 days and above), and a proliferative phase (28 days and later). MDV causes severe immune suppression characterized by prolonged thymic and bursal atrophy (Calnek *et al.*, 1998), and a variety of inflammatory neurological syndromes such as nerve enlargements and classical transient paralysis (Witter *et al.*, 1999). The exact molecular mechanism for the above-mentioned pathological conditions are unknown, it is established that a correlation exists between virulence of a strain and its prolonged cytolytic infections (Jarosinski *et al.*, 2005).

Although the natural route of MDV infection is through the respiratory tract, we chose to use intraperitoneal route to infect chicks in this experiment. In nature, during the proliferation stage of the virus cycle, the virus is transported to the feather follicles by T lymphocytes and enters the environment as dander. This dander is infective and when inhaled by susceptible birds and causes MD. The natural route of MDV infection was not chosen in this study due to inability to deliver precise quantities of MDV to the birds using dander, which have resulted in large variations and thus more complexity in the interpretation of results. As MDV targets the immune system, specifically T lymphocytes, the manifestation of the disease to alter the immune system is likely due to the established link between the immune system and microbiome. Due to this microorganisms-immune link, we feel that irrespective of the origin of virus entry, the microbiota of the chicks will be affected due to MDV.

Based on our results, MDV has an influence on the total core gut flora in chicken at the early cytolytic phase (2–7 days) and in the late proliferative phase (28–35 days) in the cecum samples. We validated the presence of MDV genomes in both the cecum and splenic tissue from both MDV-infected and uninfected chicks thus providing further evidence on the effect of MDV on the cecum. MDV infects both B and T lymphocytes in the early cytolytic phase, with significantly more B cells infected than T cells. The infected B cells then activate the T cells, thereby making them available for infection (Calnek *et al.*, 1984a). Moreover, during the early cytolytic phase, events such as the production of viral proteins such as pp38 and the integration of viral genome to the host have been shown to occur in most secondary lymphoid tissue such as the GALT and cecum tonsils (Baigent & Davison, 2004). There was no correlation between the MDV copy number between the cecum and spleen samples. This absence in correlation between the two tissue types (spleen vs. cecum) could be due to the disparity in the size of these organs, and relative composition of these tissues.

We chose the cecum as a specific site for studying the influence of MDV due to the presence of a specific immune tissue of the GALT system, namely cecal tonsils, forming a strategic immunological gateway for the transport of food, movement of microorganisms, and immune cells. Early sampling of the cecum was not possible due to logistics and the size of the chicks. The cecum samples showed no differences in community structure in the middle sampling points of the infection (14–21 days). Late sampling time points (28–35 days) formed two distinct groups (Fig. 6, groups 2 and 3) that clustered well within the infection status, providing evidence that there were differences in the community structure in the ceca. At 28–35 days, the virus is in its proliferative cycle, ready to spread to new hosts and cause reinfection. Due to the immune suppressive and inflammatory aspect of MDV, changes in the cecal microbiome could be delayed due to the viral replicative cycle. Another possibility could be a

delayed reaction caused by the immune system to account for the necessary changes to the microbial communities of the cecum. We are presently looking at the gene expression in the cecal tonsils as a complement of viral infection.

In mammals, the phylum *Firmicutes* is associated with regulation of the inflammatory immune response (Atarashi *et al.*, 2013). We observed changes in this phylum that are suggestive that a similar regulation may occur in the chicken immune system. Based on mouse models, microbiota is thought to play an important role in the $CD4^+$ T-cell differentiation. During an infection, microbial and host signals provide the necessary signal to naïve $CD4^+$ T cells to induce their differentiation into various pro- and anti-inflammatory subsets. For example, infection by intracellular pathogens drives the development of T helper cells (Th1), whereas extracellular pathogens induce the differentiation of Th2 and Th17 subsets of the T-cell population (Bettelli *et al.*, 2006; Lee & Mazmanian, 2010). During microbial infection, the activity of the immune system and especially the T cells are controlled by regulatory T cells (T_{regs}). Furthermore, T_{regs} are regulated by a specific transcription factor, Foxp3 (forkhead box P3) that induces regulatory phenotypes and functions by $CD4^+$ T cells (Fontenot *et al.*, 2005). Although chicken has been a classical developmental biology and immunity model, especially for B cells, little is known about T-cell regulation and the role of T_{regs} due to the absence of Foxp3-like sequences, leading one to assume that other similar regulatory factors have to be present that act as analogues for the control of T cells. Perhaps, induction of immune regulatory mechanisms in response to MDV induced inflammation creates a niche for the microbiota differences we observed in the infected chicks. As MDV induces T-cell lymphomas, our data suggest that by destroying T cells, the GI tract provides the perfect environment for nonspecific colonization, which in our case occurs with phylum *Proteobacteria*, at the early stages of infection when compared to uninfected birds (phylum *Firmicutes*).

There is limited literature on dysbiosis caused by viruses, but a recent study on the influence of simian immunodeficiency virus (SIV) on the chimp microbiome showed the selective enrichment of few phylotypes in the gut flora after infection (Moeller *et al.*, 2013). There are many similarities with the present study in which MDV was used to cause dysbiosis in the gut flora leading to selection of few choice species of genera *Lactobacillus*. Although MDV and SIV are different viruses (DNA herpesvirus and RNA retrovirus, respectively), they do have some similar lines of pathogenicity such as immunosuppression and influence of inflammation. Both these viruses (SIV and MDV) attack T cells and decimate the immune system of the host, leading to secondary changes in immune function, which affects the gut microbiome of the host. Furthermore, infection by MDV leads to more abundant OTUs in the infected samples compared with the uninfected samples due to the availability of new and expansion of old niches, as seen in the SIV and chimp model (Moeller *et al.*, 2013). The similarities end there due to the differences in intensities of infection, pathogenesis, and life cycles of these viruses.

MDV pathogenesis provides the necessary framework for dysbiosis to occur in the chicken gut flora leading to the enrichment of certain bacterial genera in total and cecum of the birds. These phylotypes were *Lactobacillus* (facultative anaerobic, rod-shaped bacterium), which was present in both the total fecal and cecum samples and *Haemophilius* (Gram-negative, coccobacilli bacteria) associated with the total fecal samples. *Lactobacillus* are Gram-positive, facultative anaerobic rod-shaped bacteria that are present in the GI tract in small numbers and produce probiotic regulators (Altermann *et al.*, 2005) that could help the host. *Haemophilius* have not been associated with the production of effector molecules but are regarded as commensals in the gut, with the exception of a few pathogenic strains, such as *Haemophilius influenza.*

To see whether the *Lactobacillus* sp. from two populations (total fecal vs. cecum samples) were identical, we did a phylogenetic analysis of the sequences using clustalW (Thompson *et al.*, 1994). The sequences fell into more than four groups, suggesting more than one type of *Lactobacillus* species present in the chicken gut (data not shown). Although traditionally *Lactobacillus* sp. has been reported as a probiotic in the products such as yogurt, there have been many reported cases in which *Lactobacillus* sp. has been associated with infections (Cannon *et al.*, 2005), suggesting the possibility that these strains of genus *Lactobacillus* could be an opportunistic pathogen that proliferates under a weakened immune system. Isolation of these strains using traditional culture techniques could shed light on the physiology and infective status of these strains.

In the present study, using experimental inbred layer birds as a model, NGS data reveals most sequences are associated with phyla *Firmicutes* and *Proteobacteria* with very few (< 10%) sequences found to be associated with other phyla or unclassified in total and cecum samples. Phyla *Bacteroides*, which are predominantly found in most GI studies, were under represented in both the total and cecum samples of the chicken. In most samples (total or cecum), irrespective of days, phylum *Bacteroides* represented < 1% of the total sequences and therefore did not make up the final data analysis.

In conclusion, the present study sheds light into the relative new field of dysbiosis caused by virus on the host

microbiome. The results presented in this study, show dysbiosis to occur in the chicken gut flora due to MDV infection. The change to the microbial population correlates well with the early infectious stage of MDV and the proliferation stage of the virus. Moreover, there was a specific enrichment of few select genera due to the infection status of the birds. Due to the complexity of the viral life cycle and the GALT system of the host, it is difficult to pinpoint the exact mode of action of the virus on the microbiome, or if there was a direct or indirect effect of either the virus or immune system mediated. Furthermore, microbiome changes to MDV occur in compartmentalized regions of the digestive system, like the ceca. A more thorough examination of the different regions of the chick gut could serve as a valid point of research sampling in the future that could lead to the identification of select microorganisms useful in diagnosis of MD in chicken. More work is presently being undertaken to dissect the role of cecal microbial communities and the GALT immune system using a larger and more diverse approach.

Acknowledgements

We thank Laurie Molitor for excellent technical assistance, Spencer Jackson for assistance with DNA extraction from chicken samples, preparation of samples for sequencing, and qPCR analysis. This project was supported by Agriculture and Food Research Initiative Competitive Grant no. 2012-67015-19419 from the USDA National Institute of Food and Agriculture.

References

Altermann E, Russell WM, Azcarate-Peril MA *et al.* (2005) Complete genome sequence of the probiotic lactic acid bacterium *Lactobacillus acidophilus* NCFM. *P Natl Acad Sci USA* **102**: 3906–3912.

Arpaia N, Campbell C, Fan X *et al.* (2013) Metabolites produced by commensal bacteria promote peripheral regulatory T-cell generation. *Nature* **504**: 451–455.

Atarashi K, Tanoue T, Oshima K *et al.* (2013) T_{reg} induction by a rationally selected mixture of *Clostridia* strains from the human microbiota. *Nature* **500**: 232–236.

Baigent SJ & Davison F (2004) Marek's disease virus: biology and life cycle. *Marek's Disease an Evolving Problem* (Davison F & Nair V, eds), pp. 62–78. Elsevier, Oxford, UK.

Benson A, Pifer R, Behrendt CL, Hooper LV & Yarovinsky F (2009) Gut commensal bacteria direct a protective immune response against *Toxoplasma gondii*. *Cell Host Microbe* **6**: 187–196.

Bettelli E, Carrier Y, Gao W, Korn T, Strom TB, Oukka M, Weiner HL & Kuchroo VK (2006) Reciprocal developmental pathways for the generation of pathogenic effector TH17 and regulatory T cells. *Nature* **441**: 235–238.

Calnek BW, Schat KA, Ross LJ & Chen CL (1984a) Further characterization of Marek's disease virus-infected lymphocytes. II. *In vitro* infection. *Int J Cancer* **33**: 399–406.

Calnek BW, Schat KA, Ross LJ, Shek WR & Chen CL (1984b) Further characterization of Marek's disease virus-infected lymphocytes. I. *In vivo* infection. *Int J Cancer* **33**: 389–398.

Calnek BW, Harris RW, Buscaglia C, Schat KA & Lucio B (1998) Relationship between the immunosuppressive potential and the pathotype of Marek's disease virus isolates. *Avian Dis* **42**: 124–132.

Cannon JP, Lee TA, Bolanos JT & Danziger LH (2005) Pathogenic relevance of *Lactobacillus*: a retrospective review of over 200 cases. *Eur J Clin Microbiol Infect Dis* **24**: 31–40.

Caporaso JG, Bittinger K, Bushman FD, DeSantis TZ, Andersen GL & Knight R (2010a) PyNAST: a flexible tool for aligning sequences to a template alignment. *Bioinformatics* **26**: 266–267.

Caporaso JG, Kuczynski J, Stombaugh J *et al.* (2010b) QIIME allows analysis of high-throughput community sequencing data. *Nat Methods* **7**: 335–336.

DeSantis TZ, Hugenholtz P, Larsen N, Rojas M, Brodie EL, Keller K, Huber T, Dalevi D, Hu P & Andersen GL (2006) Greengenes, a chimera-checked 16S rRNA gene database and workbench compatible with ARB. *Appl Environ Microbiol* **72**: 5069–5072.

Edgar RC (2010) Search and clustering orders of magnitude faster than BLAST. *Bioinformatics* **26**: 2460–2461.

Egan CE, Cohen SB & Denkers EY (2012) Insights into inflammatory bowel disease using *Toxoplasma gondii* as an infectious trigger. *Immunol Cell Biol* **90**: 668–675.

Fontenot JD, Rasmussen JP, Gavin MA & Rudensky AY (2005) A function for interleukin 2 in Foxp3-expressing regulatory T cells. *Nat Immunol* **6**: 1142–1151.

Gimeno IM, Cortes AL & Silva RF (2008) Load of challenge Marek's disease virus DNA in blood as a criterion for early diagnosis of Marek's disease tumors. *Avian Dis* **52**: 203–208.

Gloor GB, Hummelen R, Macklaim JM, Dickson RJ, Fernandes AD, MacPhee R & Reid G (2010) Microbiome profiling by illumina sequencing of combinatorial sequence-tagged PCR products. *PLoS ONE* **5**: e15406.

Hamady M, Walker JJ, Harris JK, Gold NJ & Knight R (2008) Error-correcting barcoded primers for pyrosequencing hundreds of samples in multiplex. *Nat Methods* **5**: 235–237.

Hess M, Sczyrba A, Egan R *et al.* (2011) Metagenomic discovery of biomass-degrading genes and genomes from cow rumen. *Science* **331**: 463–467.

Hooper LV, Falk PG & Gordon JI (2000) Analyzing the molecular foundations of commensalism in the mouse intestine. *Curr Opin Microbiol* **3**: 79–85.

Hooper LV, Wong MH, Thelin A, Hansson L, Falk PG & Gordon JI (2001) Molecular analysis of commensal host-microbial relationships in the intestine. *Science* **291**: 881–884.

Jarosinski KW, Njaa BL, O'connell PH & Schat KA (2005) Pro-inflammatory responses in chicken spleen and brain

tissues after infection with very virulent plus Marek's disease virus. *Viral Immunol* **18**: 148–161.

Kim HB, Borewicz K, White BA, Singer RS, Sreevatsan S, Tu ZJ & Isaacson RE (2012) Microbial shifts in the swine distal gut in response to the treatment with antimicrobial growth promoter, tylosin. *P Natl Acad Sci USA* **109**: 15485–15490.

Lee YK & Mazmanian SK (2010) Has the microbiota played a critical role in the evolution of the adaptive immune system? *Science* **330**: 1768–1773.

Ley RE, Backhed F, Turnbaugh P, Lozupone CA, Knight RD & Gordon JI (2005) Obesity alters gut microbial ecology. *P Natl Acad Sci USA* **102**: 11070–11075.

Lillehoj HS & Trout JM (1996) Avian gut-associated lymphoid tissues and intestinal immune responses to Eimeria parasites. *Clin Microbiol Rev* **9**: 349–360.

Looft T, Johnson TA, Allen HK *et al.* (2012) From the Cover: in-feed antibiotic effects on the swine intestinal microbiome. *Proc Natl Acad Sci* **109**: 1691–1696.

Lozupone C & Knight R (2005) UniFrac: a new phylogenetic method for comparing microbial communities. *Appl Environ Microbiol* **71**: 8228–8235.

Marchesi JR, Dutilh BE, Hall N, Peters WH, Roelofs R, Boleij A & Tjalsma H (2011) Towards the human colorectal cancer microbiome. *PLoS ONE* **6**: e20447.

Mazmanian SK, Liu CH, Tzianabos AO & Kasper DL (2005) An immunomodulatory molecule of symbiotic bacteria directs maturation of the host immune system. *Cell* **122**: 107–118.

Mazmanian SK, Round JL & Kasper DL (2008) A microbial symbiosis factor prevents intestinal inflammatory disease. *Nature* **453**: 620–625.

Minot S, Sinha R, Chen J, Li H, Keilbaugh SA, Wu GD, Lewis JD & Bushman FD (2011) The human gut virome: inter-individual variation and dynamic response to diet. *Genome Res* **21**: 1616–1625.

Moeller AH, Shilts M, Li Y, Rudicell RS, Lonsdorf EV, Pusey AE, Wilson ML, Hahn BH & Ochman H (2013) SIV-induced instability of the chimpanzee gut microbiome. *Cell Host Microbe* **14**: 340–345.

Molloy MJ, Grainger JR, Bouladoux N *et al.* (2013) Intraluminal containment of commensal outgrowth in the gut during infection-induced dysbiosis. *Cell Host Microbe* **14**: 318–328.

Morrow C & Fehler F (2004) Marek's disease: a worldwide problem. *Marek's Disease: An Evolving Problem* (Davison F & Nair V, eds), pp. 49–61. Elsevier, Oxord, UK.

Okulewicz A & Zlotorzycka J (1985) Connections between *Ascaridia galli* and the bacterial flora in the intestine of hens. *Angew Parasitol* **26**: 151–155.

Price MN, Dehal PS & Arkin AP (2009) FastTree: computing large minimum evolution trees with profiles instead of a distance matrix. *Mol Biol Evol* **26**: 1641–1650.

Qu A, Brulc JM, Wilson MK *et al.* (2008) Comparative metagenomics reveals host specific metavirulomes and horizontal gene transfer elements in the chicken cecum microbiome. *PLoS ONE* **3**: e2945.

Round JL & Mazmanian SK (2010) Inducible Foxp3+ regulatory T-cell development by a commensal bacterium of the intestinal microbiota. *P Natl Acad Sci USA* **107**: 12204–12209.

Saengkerdsub S, Anderson RC, Wilkinson HH, Kim WK, Nisbet DJ & Ricke SC (2007) Identification and quantification of methanogenic Archaea in adult chicken ceca. *Appl Environ Microbiol* **73**: 353–356.

Schat KA & Nair V (2008) Marek's disease. *Disease of Poultry* (Saif YM, Fadly AM, Glisson JR, McDouglad LR, Nolan LK & Swayne DE, eds), pp. 452–514. Blackwell, Ames, IA.

Schloss PD, Westcott SL, Ryabin T *et al.* (2009) Introducing mothur: open source, platform-independent, community-supported software for describing and comparing microbial communities. *Appl Environ Microbiol* **75**: 7537–7541.

Scupham AJ (2007) Examination of the microbial ecology of the avian intestine *in vivo* using bromodeoxyuridine. *Environ Microbiol* **9**: 1801–1809.

Spor A, Koren O & Ley R (2011) Unravelling the effects of the environment and host genotype on the gut microbiome. *Nat Rev Microbiol* **9**: 279–290.

Thompson JD, Higgins DG & Gibson TJ (1994) CLUSTAL W: improving the sensitivity of progressive multiple sequence alignment through sequence weighting, position-specific gap penalties and weight matrix choice. *Nucleic Acids Res* **22**: 4673–4680.

Wang Q, Garrity GM, Tiedje JM & Cole JR (2007) Naive Bayesian classifier for rapid assignment of rRNA sequences into the new bacterial taxonomy. *Appl Environ Microbiol* **73**: 5261–5267.

Witter RL, Gimeno IM, Reed WM & Bacon LD (1999) An acute form of transient paralysis induced by highly virulent strains of Marek's disease virus. *Avian Dis* **43**: 704–720.

Yu Z & Morrison M (2004) Improved extraction of PCR-quality community DNA from digesta and fecal samples. *Biotechniques* **36**: 808–813.